Conformation fluctuations of polymerized vesicles in the inextensible and flexible limit

Hyoungsoo Yoon* and J. M. Deutsch
Physics Department, University of California, Santa Cruz, Santa Cruz, California 95064
(Received 23 December 1996)

We study conformation fluctuations of a tethered membrane of spherical shape. The membrane is assumed to be both inextensible and flexible. We first study linear fluctuations and show that they are irrelevant in this limit. Nonlinear fluctuations can be described in terms of isometric buckling of local circular portions of the membrane. Configurations of buckled regions on the membrane are then modeled as a system of rings whose excitation energies are the elastic energy cost of buckling. The rings should be nonoverlapping with one another due to geometrical constraints. We study the thermodynamics of this system using a variational method, and the results are interpreted in terms of the shape fluctuations of the membrane itself. Our results indicate that there is no roughening transition when we raise the temperature. In other words, the membrane remains ''flat'' at all temperatures even though it is made of very flexible material. [S1063-651X(97)02209-5]

PACS number(s): 87.22.Bt, 05.20−y, 02.40.Hw

I. INTRODUCTION

Over the last several years, polymerized or tethered membranes [1–4] have been extensively studied, partly due to their relevance to the biophysics of cell membranes [5]. Mammalian red blood cells, for example, have lipid bilayer membranes with cross-linked spectrin networks anchored, which play important roles in determining the equilibrium shapes and the fluctuations around them [6]. The spectrin networks have been extracted and their fluctuations have been investigated by various experimental methods [7,8], giving slightly ambiguous results, especially regarding the presence of the so-called *crumpled phase* [9–15]. Cross-linked synthetic polymer networks [16] or exfoliated graphite oxide crystals [17,18] have also been used in experiments.

In theoretical studies, polymerized membranes are usually modeled as elastic sheets, since microscopic details will be irrelevant on large length scales. The mesh size of spectrin networks, for example, is of order 10^{-7} m, but often we are interested in fluctuations on the order of 10^{-5} m. In this case, membranes can be idealized as purely two-dimensional surfaces with bending rigidities, in-plane shear, and compressional moduli [19,20].

The energies due to in-plane strain are, in general, much larger than those from bending, as will be illustrated shortly for cases of thin elastic sheets and red blood cell membranes. Hence, if bending without stretching or shearing is allowed, it will dominate the low-temperature fluctuations. However, stretching almost always accompanies bending except, for example, when flat elastic sheets are rolled [21]. Hence, in general, the undulations which *localize* stretched or sheared areas will be the dominant modes.

This type of shape deformations was first studied by Lobkovsky *et al.* [22] for membranes whose ground-state shapes are flat. For flat membranes the above argument applies only for large-amplitude fluctuations or forced crumpling, since the in-plane strain is second order in bending amplitudes and hence in-plane modes are irrelevant in the harmonic approximation. However, the situation is different for ''curved'' membranes, for which stretching or shearing modes are the same order effects as those from out-of-plane undulations. Polymerized vesicles [23–26], for example, cannot bend without stretching. This is purely for geometrical reasons, and this behavior of closed surfaces becoming very inflexible due to slight stretchability is known as the monotypy theorem in classical elasticity theory [19].

Let us consider an elastic membrane which has a shape of a spherical shell in its undeformed state. Suppose we apply an external force at one point on the surface. If it is perfectly inextensible, then, even though it is extremely flexible, it would not allow any deformation for the reason just discussed. Now, if we add a slight extensibility along with a finite flexibility, it will make a small circular dent when acted on by an external force. The size of the dent will be determined by the competition between the two energy terms, bending and stretching: The more flexible and the more inextensible the material is, the smaller the size will be. For a small enough force the size of the dent is almost constant, but when we increase the force beyond a certain critical value the surface will buckle [27] and the size of the dimple will grow. We claim that this dimplelike localized deformation of circular shape is the most relevant one in describing the fluctuations of spherical membranes, which are very inextensible and flexible at the same time.

We focus in this paper on such shape changes of curved membranes due either to external forces or to thermal fluctuations. For mathematical simplicity we restrict ourselves to membranes with constant radii of curvature, i.e., closed spherical shells. The membranes are assumed to be *inextensible* (or *incompressible*) and *flexible*, that is, the characteristic in-plane elastic energy is supposed to be much larger than the typical bending energy. It should be noted that this is the complementary limit of that usually studied through renormalization-group methods. The in-plane moduli are known to be renormalized to zero at large length scales, while the bending rigidity diverges due to its nonlinear coupling with in-plane phonon modes [2–4,9]. This implies that the membrane is in the flat (noncrumpled) phase. Therefore

*Present address: Basic Science Research Institute, Postech, Pohang, Korea 790-784.

our model should be considered with the understanding that it provides a valid description of fluctuation of membranes only below a certain length scale and at low enough temperatures. This will be explained later in more quantitative terms.

The outline of this paper is as follows. In Sec. II, we first review some basics of classical elasticity theory for two-dimensional surfaces suitable for a statistical mechanics approach. We then present precise definitions of inextensibility and floppiness, and their limits of validity are clarified. This section provides the motivation for our study of inextensible and flexible membranes. Both linear and nonlinear conformation changes due to external forces are discussed in Sec. III, which will be the basis for the main argument of this paper.

In Sec. IV, the forced crumpling of spherical membranes in various circumstances will be described. We will restrict our discussion to nonsingular deformations throughout this paper. This nonlinear and nonsingular regime is only possible because of the initial curvature in the membranes. For flat membranes, large deformation (other than simple rolling or corrugation) immediately introduces singularities as described by Lobkovsky *et al.* [22]. The elastic energy is confined along a line joining two singular points in this case, whereas the line makes a closed loop in our case. The interaction of polymerized vesicles with smooth surfaces will also be briefly mentioned.

We then present the thermal fluctuation of closed spherical shells in Sec. V. First, we argue that dimplelike ''elementary'' excitations are the building blocks of the shape fluctuations. Then we formulate a statistical mechanical problem of nonoverlapping dimples, and solve it through a variational method. We show that the membrane remains ''flat'' due to the interactions between these dimples in the suitable limit. Finally, in Sec. VI we summarize our results and present directions for future research.

II. MODEL

We consider a closed elastic membrane with a constant radius of curvature R, i.e., a hollow spherical shell. The membrane is assumed to be very inextensible and very flexible at the same time. We assume that it has a small but finite thickness t, which is uniform throughout the surface.

Any two-dimensional geometric surfaces embedded in three-dimensional Euclidean space can be characterized by two bilinear functions: the first fundamental form, i.e., the induced metric tensor, and the second fundamental form, which represents the extrinsic geometry of the surface [28]. Therefore the elastic energy of a thin membrane, in the limit of $t \to 0$, can be idealized to consist of two separate contributions: one from the in-plane strain and the other from its bending in three-dimensional Euclidean space [20].

We use, throughout this paper, a local coordinate system around an arbitrarily chosen point on a membrane such that it is the projection of the Cartesian coordinate system of the tangent plane to the undeformed membrane at that point (Monge representation). We use $\vec{\lambda}=(\lambda_x,\lambda_y)=(x,y)$ to represent the internal coordinate on the membrane, then, in this coordinate system, the first and the second fundamental forms $G_{\alpha\beta}$ and $B_{\alpha\beta}$ are represented as

$$G_{\alpha\beta}=\begin{pmatrix}1 & 0\\ 0 & 1\end{pmatrix}, \tag{1}$$

$$B_{\alpha\beta}=\begin{pmatrix}\frac{1}{R} & 0\\ 0 & \frac{1}{R}\end{pmatrix}, \tag{2}$$

where we have assumed that R is much larger than the size of the coordinate patch, which is in turn much larger than the typical length scale in the problem.

We use $\vec{u}=(u_x,u_y)$ to denote the tangential displacement, and w to denote the vertical (*inward*) deflection of the membrane from this ground-state conformation. In general, the magnitude of $\vec{u}$ will be very small compared to w, because the membrane is assumed to be very inextensible. The in-plane strain tensor $u_{\alpha\beta}$ and the bending strain tensor $w_{\alpha\beta}$ are represented, to the lowest order, by

$$u_{\alpha\beta}=\frac{1}{2}\left(\frac{\partial u_\alpha}{\partial\lambda_\beta}+\frac{\partial u_\beta}{\partial\lambda_\alpha}-2B_{\alpha\beta}w\right)+\frac{1}{2}\frac{\partial w}{\partial\lambda_\alpha}\frac{\partial w}{\partial\lambda_\beta} \tag{3}$$

and

$$w_{\alpha\beta}=-\frac{\partial^2 w}{\partial\lambda_\alpha\partial\lambda_\beta}. \tag{4}$$

Here, and throughout this paper, Greek letters such as α and β are used to denote x and y components of the two-dimensional vectors. Note that the coordinate patch should be small enough so that $\partial w/\partial\lambda_\alpha$ is always bounded for both $\alpha=x$ and y.

The elastic energy densities F_S and F_B due to stretching and bending, respectively, are given, up to the second order, as follows (Hooke's law):

$$f_S=\tfrac{1}{2}k_{S1}(\mathrm{Tr}\ u_{\alpha\beta})^2+k_{S2}\mathrm{Tr}(u_{\alpha\beta})^2, \tag{5}$$

$$f_B=\tfrac{1}{2}k_{B1}(\ \mathrm{Tr}\ w_{\alpha\beta})^2+k_{B2}\ \mathrm{Tr}(w_{\alpha\beta})^2, \tag{6}$$

where the coefficients are the two-dimensional elastic constants, whose physical meanings are

$$k_S=k_{S1}+k_{S2}\quad \text{bulk modulus},$$

$$k_{S2}\quad \text{shear modulus},$$

$$k_B=k_{B1}+2k_{B2}\quad \text{bending rigidity},$$

$$2k_{B2}\quad \text{Gaussian rigidity}.$$

Note that the Gaussian rigidity term of f_B ($\sim \mathrm{Det}\, w_{\alpha\beta}$) can be safely neglected for closed membranes from the Gauss-Bonnet theorem [28].

When the membrane is made of a homogeneous material with (three-dimensional) Young's modulus E and Poisson ratio σ, these constants are expressed as follows [19]:

$$k_{S1}=\frac{\sigma E t}{1-\sigma^2}, \tag{7}$$

$$k_{S2}=\frac{Et}{2(1+\sigma)}, \tag{8}$$

$$k_{B1}=\frac{\sigma E t^3}{12(1-\sigma^2)}, \tag{9}$$

$$k_{B2}=\frac{Et^3}{24(1+\sigma)}. \tag{10}$$

Note that $k_{S1}\approx k_{S2}$ and $k_{B1}\approx k_{B2}$, since σ is a small positive number ($\lesssim 1/2$) for most materials. This is generally true for other inhomogeneous membranes such as biomembranes. Since we are mainly interested in the relative importance of stretching and bending contributions to the elastic energy, we will only use two symbols k_S and k_B to represent the typical sizes of the in-plane modulus and the bending rigidity, respectively, unless otherwise indicated.

From the above expressions, it is easy to see that the bending moduli become quadratically smaller in t relative to the in-plane moduli as $t\to 0$; that is to say, the membrane is more inextensible than rigid-to-bending as its thickness becomes small. For our polymerized membranes of interest, whose lateral dimensions are typically much larger than the thickness, this is usually true as well. For mammalian red blood cell membranes of thickness $t\sim 10^{-8}$ m, k_B is around 10^{-20} J, whereas k_S is around 10^{-2} N/m. Even though the thickness is fixed for this case, the numbers indicate that k_B is about t^2 times larger than k_S.

The total energy is obtained by integrating the sum of f_S and f_B over the entire surface,

$$F[\vec{u},w]=\int_{\text{membrane}} d\vec{\lambda}(f_S+f_B), \tag{11}$$

where the invariant integration measure has been substituted by that of the undeformed sphere, $\sqrt{\text{Det}(G_{\alpha\beta})}d\vec{\lambda}$, which is none other than that of a plane, $d\vec{\lambda}$. This integration has to be done in many coordinate patches.

The fluctuations of elastic membranes can be studied, in principle, by calculating the partition function Z from this ''Hamiltonian,'' F,

$$Z=\int DM[\vec{u},w]e^{-\beta F[\vec{u},w]}, \tag{12}$$

where the functional integration measure $DM[\vec{u},w]$ includes the self-avoiding constraint, and β is the inverse temperature, in units of the Boltzmann constant. In general, calculating Z is a formidable task, if not impossible. In this paper, we restrict ourselves to a special class of membranes which are inextensible and flexible, whose meanings will become clear in the following discussion.

Let us first estimate the relative importance of the two terms in the elastic energy, Eq. (11). If an initially flat membrane *warps* about w over an arbitrary length scale l, then $|u_{\alpha\beta}|$ is of order w^2/l^2 and $|w_{\alpha\beta}|$ of order w/l^2 from Eqs. (3) and (4). Therefore, from Eqs. (5) and (6),

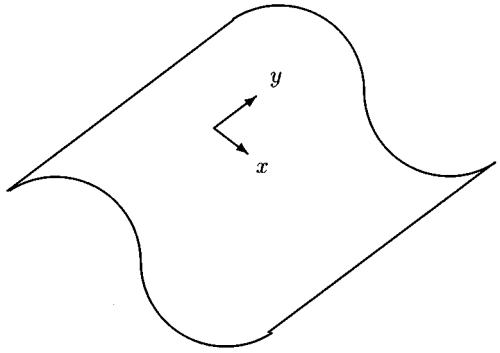

FIG. 1. Corrugation of a planar membrane in the x direction. This is the only mode of deformation for completely inextensible membranes.

$$\frac{f_S}{f_B}\approx\frac{k_S}{k_B}w^2. \tag{13}$$

For the case of membranes made of homogeneous material, $k_S/k_B\sim t^{-2}$ as explained earlier, and hence $f_S/f_B\sim w^2/t^2$. Since we are interested in large length scale fluctuations, i.e., we assume that l is large enough such that $w^2\gg t^2$ (or $w^2\gg k_S/k_B$, in general) in this paper, the above argument justifies our study of membranes which are inextensible ($f_S\to\infty$) and flexible ($f_B\to 0$). Below a certain length scale l_c, however, the bending energy always dominates the in-plane energy. Without this length scale $l_c\sim\sqrt{k_B/k_S}$ or $\sim t$, the membrane would become too rough to be described by classical elasticity theory. This small-scale smoothness also makes it possible to take the local coordinate systems defined earlier.

If we consider large deformations which are comparable to the linear size of membranes, that is $w\approx l$, such as in the case where a flat membrane is bent into hemispherical shell, the ratio f_S/f_B for homogeneous membranes is just the square of the aspect ratio between the linear size and the thickness, which can be as large as 1000 in most cases of interest, yielding $f_S/f_B=10^6$. We also obtain similar figures for cell membranes of typical size $R\sim 10^{-4}$ m.

For a *planar* membrane ($R\to\infty$), however, deformations without stretching are possible, and hence these fluctuations will be dominant modes at low temperatures. The complete inextensibility imposes the constraints $u_{\alpha\beta}=0$, that is,

$$2\frac{\partial u_x}{\partial x}+\left(\frac{\partial w}{\partial x}\right)^2=0, \tag{14}$$

$$2\frac{\partial u_y}{\partial y}+\left(\frac{\partial w}{\partial y}\right)^2=0, \tag{15}$$

$$\frac{\partial u_x}{\partial y}+\frac{\partial u_y}{\partial x}+\frac{\partial w}{\partial x}\frac{\partial w}{\partial y}=0 \tag{16}$$

in an appropriate coordinate system. The only allowed solutions are simple corrugations of a membrane [21] as shown in Fig. 1. For curved membranes, this mode of fluctuation is

not allowed due to geometrical constraints, and the bending and the stretching modes are *always* coupled as will be discussed in Sec. III.

III. SHAPE DEFORMATIONS

A. Linear regime

Elasticity theory is usually nonlinear from two origins, physical and geometrical. Since we always assume physical linearity in this paper, that is, the material is assumed to obey Hooke's law [Eqs. (5) and (6)], the reason why the model partition function Eq. (12) leads to the nonlinear equations of state is purely geometrical.

Let us also assume geometrical linearity in this subsection, which, in particular, implies assuming a very large R. Then we can neglect the nonlinear terms in the strain tensors $u_{\alpha\beta}$ and $w_{\alpha\beta}$. We further assume that u_x and u_y are so small that we can neglect them entirely. Then we have only one scalar field of displacement on the sphere, w. Now we can easily compute the partition function for this system. First, in the local Cartesian coordinate system defined in Sec. II, the strain tensors become

$$u_{\alpha\beta}=\begin{pmatrix} -\frac{w}{R} & 0 \\ 0 & -\frac{w}{R} \end{pmatrix} \tag{17}$$

and

$$w_{\alpha\beta}=\begin{pmatrix} -\frac{\partial^2 w}{\partial x^2} & -\frac{\partial^2 w}{\partial x \partial y} \\ -\frac{\partial^2 w}{\partial x \partial y} & -\frac{\partial^2 w}{\partial y^2} \end{pmatrix}. \tag{18}$$

From Eqs. (5), (6), and (11), it is easy to obtain

$$\begin{aligned} F &= \int d\vec{\lambda}\left[\frac{2k_S}{R^2}w^2+\frac{k_B}{2}(\vec{\nabla}^2 w)^2\right] \\ &= \tfrac{1}{2}\int d\vec{\lambda} w\left(\frac{4k_S}{R^2}+k_B\vec{\nabla}^4\right)w, \end{aligned} \tag{19}$$

where k_S and k_B were defined in Sec. II. Then the height-height correlation function is easily obtained [29]:

$$\begin{aligned} \langle w(\vec{\lambda})w(\vec{0})\rangle &= \frac{1}{(2\pi)^2}\frac{1}{\beta}\int d\vec{q}\,\frac{e^{i\vec{q}\cdot\vec{\lambda}}}{\frac{4k_S}{R^2}+k_B\vec{q}^4} \\ &\approx -\frac{4}{\pi}\langle w^2\rangle \,\mathrm{kei}\left(\frac{|\vec{\lambda}|}{\xi}\right), \end{aligned} \tag{20}$$

where kei(x) is a Kelvin function of zeroth order, which is $-\pi/4$ at the origin and decays rapidly (oscillating) to zero beyond $x\sim 1$ [30]. Note that the phonons (the *bending waves*) become massive due to the nonzero curvature of the initial conformation. Its characteristic length scale is given by

$$\xi\approx\left(\frac{k_B}{k_S}\right)^{1/4}R^{1/2}\approx(tR)^{1/2}, \tag{21}$$

which is around 10^{-6} m using the numbers given earlier. The on-site fluctuation of the radial displacement, defined by Eq. (20), is

$$\langle w^2\rangle\approx\frac{1}{\beta}\frac{R}{(k_Bk_S)^{1/2}}\approx\frac{1}{\beta}\frac{R}{Et^2}. \tag{22}$$

Here and throughout this paper, constants of order unity are omitted. Note that the root-mean-square fluctuation $\sqrt{\langle w^2\rangle}$ grows with the exponent $\frac{1}{2}$ as the radius R increases. Hence the linear fluctuation will be irrelevant for a large spherical membrane. However, more importantly, the linear theory breaks down when the free-energy contribution from the last term in Eq. (3) becomes comparable to that of the linear order, at which point the amplitude of the radial fluctuation $\sqrt{\langle w^2\rangle}$ is of the order ξ^2/R. That is, the following should hold,

$$R\beta^{-1}\ll\left(\frac{k_B^3}{k_S}\right)^{1/2}\approx Et^4, \tag{23}$$

in order for the linear theory to be applicable. The typical value of the right-hand side is around 10^{-28} J m. This translates, for a spherical membrane with $R=10^{-4}$ m, into a critical temperature below 1 K. Therefore we conclude that one has to go beyond the linear theory to explain the fluctuations of spherical membranes of ''typical'' size in the physically interesting limit.

A more general case without the assumption of inextensibility (or $u_x=u_y=0$) in the linear theory, was studied in Ref. [24]. In this study, the longitudinal phonon modes were found to be coupled with the radial undulations.

B. Buckling

If we retain nonlinear terms in the partition function, the radial (vertical) phonons are no longer independent, and we need to take into account the interactions among them. In fact, the interactions are so strong that perturbation theory does not work very well. Hence we will consider solitonlike excitations as described in this section. The nonlinear fluctuations of the polymerized membranes will be described in terms of this idea in Sec. V.

It should be noted first that, for curved membranes, it is no longer possible to neglect stretching completely. Otherwise, no deformations are allowed at all due to geometrical constraints (the monotypy theorem).

When we apply a localized force at one point on the sphere, it makes a small dent of radius ξ in the linear approximation, as described earlier. If we increase the strength of the applied force beyond a certain critical value, the surface will abruptly buckle, and it is no longer in the linear regime. Since the membrane is assumed to be very inextensible, any allowed deformations should be approximately

isometric transformations, i.e., a mirror transformation in this case, of a circular region of the membrane across an imaginary plane which intersects the sphere. Then, since we assume that the *spontaneous curvature* of the membrane is zero, or that the membrane is homogeneous (or symmetric) along its thickness when it is flattened, most of the elastic energy will be concentrated near the geometric edge. The width of this severely bent strip d is determined by the competition between the stretching and the bending energies, as in the linear case, and so is independent of the size of the dimple. The formation energy of a dimple can be estimated by applying a *linear* theory on this bending strip as follows [19].

Let us suppose that the applied force makes a dimple of radius r or height $h=r^2/R$. Since the displacement is localized over the width $\sim d$ along a circle of radius r, w is of order rd/R and hence $|u_{\alpha\beta}|$ is of order $(rd/R)/R$ from Eq. (3) and $|w_{\alpha\beta}|$ of order $(rd/R)/d^2$ from Eq. (4). Therefore, from Eqs. (5) and (6), the stretching energy F_S is rd times $k_S(rd/R^2)^2$, and the bending energy F_B is rd times $k_B(rd/Rd^2)^2$. That is,

$$F_S=\frac{k_S r^3 d^3}{R^4}, \tag{24}$$

$$F_B=\frac{k_B r^3}{R^2 d}. \tag{25}$$

Again, we neglect prefactors of order unity when they are not essential. By minimizing F_S+F_B with respect to d, we obtain

$$F(r)=\kappa r^3, \tag{26}$$

where

$$\kappa\approx\sqrt{k_S k_B}d/R^3\approx E(t/R)^{5/2}, \tag{27}$$

which is of order 10^{-5} N/m^2 if we use the numbers given earlier. The width of the bending strip d is the same as ξ, and this provides the minimum length scale of this problem. The formula for $F(r)$ is valid only if r is much larger than ξ. For a homogeneous membrane this translates into

$$r\gg(tR)^{1/2}. \tag{28}$$

The minimum-energy scale for buckling, $F(d)$, obtained from Eq. (26), is the same as that defined as the point where the linear theory breaks down [Eq. (23)].

In linear theory the fluctuation was symmetrical, that is, $\langle w\rangle$ was zero. The deformation due to buckling is, however, unidirectional. When we describe shape fluctuations based on this type of nonlinear deformations in Sec. V, we thus concentrate on the average height $\langle w\rangle$ rather than on its fluctuation, $\Delta w^2=\langle w^2\rangle-\langle w\rangle^2$. Note that $\langle w\rangle$ provides the upper bound for Δw due to this unidirectionality. Before we study the thermal fluctuation of the membrane due to the creation of dimples, we first present some implications of this nonlinear deformation to the mechanical properties of polymerized vesicles in Sec. IV.

IV. MECHANICAL CRUMPLING

Understanding mechanical properties of tethered vesicles is very important for various reasons: Red blood cell membranes, for example, have evolved to endure the strong flow field of the blood stream. Liposomes, used for drug delivery, will also have to be designed to stand strong stress. And there are some bacterial cells known to have tough membranes to resist high turgor pressure, which is normally controlled by cell walls in plants [31]. In this section we study some mechanical properties of the spherical membrane due to the nonlinear dimplelike deformations introduced in Sec. III. The membrane is assumed to be made of homogeneous material with mass density ρ. (Thus its mass density per unit area is $t\rho$.)

The deformation energy for a dimple of size r is given by Eq. (26) or by

$$F(h)=\overline{\kappa}h^{3/2}, \tag{29}$$

where $h=r^2/R$ is the height or vertical displacement of the dimple and $\overline{\kappa}=\kappa R^{3/2}$. When we place this sphere on the flat surface in the gravitational field g, it will buckle at the bottom due to its weight. (See Ref. [32] for different limits.) If we assume small deformation, that is, if the mass of the sphere $m=4\pi R^2 t\rho$ is small compared to $\overline{\kappa}/g$, then the equilibrium point can be found by minimizing the total energy:

$$\delta(-mgh+\overline{\kappa}h^{3/2})=0. \tag{30}$$

The equilibrium radius r_c is

$$r_c=\frac{tR\rho g}{\kappa}. \tag{31}$$

This is of order 10^{-6} m using the same parameters as in previous sections. We now neglect the gravitational effect and assume that the surface is very sticky, that is, the free energy is lowered when the sphere is in contact with the surface by the amount proportional to the area of the contact. Then

$$\delta(-\chi 2\pi rd+\kappa r^3)=0, \tag{32}$$

where χ is the adhesion coefficient. The equilibrium radius is then

$$r_c=\left(\frac{\chi d}{\kappa}\right)^{1/2}. \tag{33}$$

We next consider the interaction between two adhesive vesicles. If their strength of adhesion is proportional to the contact area as in the previous example, the equilibrium radius of a dimple turns out to be χ/κ. Hence the equilibrium distance D between the centers of the two vesicles is

$$D=2\left(R-\frac{\chi^2}{\kappa^2 R}\right). \tag{34}$$

Note that the equilibrium state is doubly degenerate due to the symmetry shown in Fig. 2. For a dense solution of these

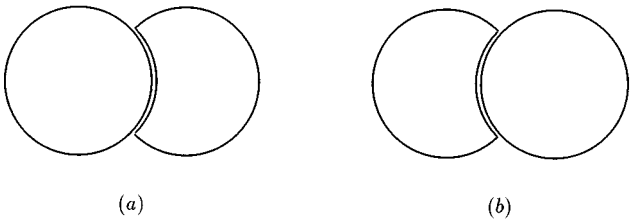

FIG. 2. Adhesion between two vesicles. Two symmetric configurations are possible with equal energy cost, as shown in (a) and (b). The sizes of the dimples are exaggerated for the sake of clarity.

spheres, or a spongelike solid phase, a residual entropy due to this degeneracy, similar to that of ice crystal, should be observable.

Finally, we consider a spherical membrane in a pressure field. For instance, we can deflate a tightly sealed membrane by sucking out the solution inside. Let us first consider the easier case of controlling the volume. If we reduce the volume inside the sphere from $V_0=\frac{4}{3}\pi R^3$ to $V<V_0$, what would be the minimum energy conformation of the sphere? Suppose there is one dimple on the surface with the radius r_1. Here r_1 can be computed from simple geometrical considerations, and it turns out that $r_1\sim(\Delta V R)^{1/4}$, where $\Delta V=V_0-V$. The energy cost to create this dimple is then $\kappa(r_1)^3\sim(\Delta V)^{3/4}$. If we had two dimples of equal size instead, then the radius r_2 would be $r_1\frac{1}{2}^{1/4}$ and hence the energy required would be increased by a factor of $2\times\frac{1}{2}^{3/4}$. That is, one large dimple is preferred over many small dimples. This is typically observed in macroscopic world, such as when we deflate a soccer ball by making a small hole on it.

Now let us apply a pressure difference p across the membrane. This can be done, for example, by changing osmotic pressure across a semipermeable membrane. Here we only consider the situation in which the outside pressure is higher than that inside the vesicle. Let us suppose, for the moment, that the membrane buckles (at one point, as in the previous paragraph) due to the applied pressure difference. Then the energy cost due to buckling will be compensated for by the work done by the pressure, that is, the total energy is

$$F=\kappa r^3-\frac{pr^4}{R}. \tag{35}$$

By minimizing this equation with respect to r, we obtain

$$r_c=\frac{\kappa R}{p}. \tag{36}$$

Since this is an unstable equilibrium, the creation of dimples will be suppressed. But dimples larger than r_c will spontaneously grow out of the valid regime of this description. The maximum pressure difference $p_{\rm cr}$ which the sphere can stand is then defined as that when r_c reaches ξ, that is,

$$p_{\rm cr}=\frac{\kappa R}{\xi}\approx\frac{Et^2}{R^2}. \tag{37}$$

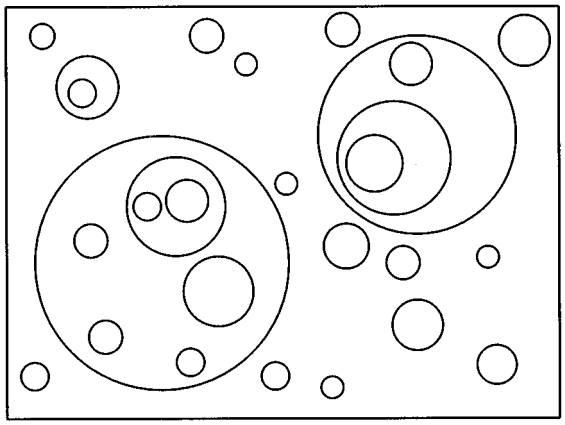

FIG. 3. A schematic picture of a typical configuration of nonoverlapping rings. The curvature of the underlying surface (membrane) is neglected, as explained in the text.

This is of order 10^{-3} N/m^2. It should be noted that this instability does not necessarily mean the total collapse of the spherical membrane when an external pressure larger than the critical one is applied.

V. THERMAL FLUCTUATIONS

A. System of hard rings

Under the assumption of strong inextensibility and flexibility, we have shown that large deformations of a closed spherical membrane can be accounted for in terms of buckling of small circular parts into their mirror images, resulting in small dimples on the surface. Since we exclude the possibility of singular deformations in this paper, no two dimples can overlap with each other. Then we can map the low-temperature phase of the fluctuation of a spherical membrane to a system of nonoverlapping dimples. Furthermore, since we are assuming that the membrane is homogeneous along its thickness, buckled regions can also accommodate other dimples which have the same sign of the radius of curvature as that of the original undeformed membrane. Then this hierarchical buckling can continue indefinitely, only to be limited by the two length scales d and R. Hence we can regard our system of dimples as that of nonoverlapping rings on a two-dimensional surface. The curvature of the underlying surface, i.e., the membrane, will be neglected, since we are interested in a length scale much smaller than the size of the vesicle, R. A schematic picture of a system of hard rings on a plane is shown in Fig. 3.

Let us then consider a system of N hard rings of width d at a fixed temperature β^{-1}. N is determined by the condition that the free energy should be at a minimum with respect to variation of N. Alternatively, one can use a grand canonical ensemble with the chemical potential set to zero because the number of rings is not conserved. The canonical partition function Z can be written as follows:

$$Z=\frac{1}{N!d^{3N}}\int\prod_{i=1}^{N}d\mu(r_i)d\vec{\lambda}_i e^{-\beta H}, \tag{38}$$

where

$$H=\sum_{i=1}^{N} F(r_i)+\sum_{i<j} U(r_i,\vec{\lambda}_i;r_j,\vec{\lambda}_j). \tag{39}$$

$F(r_i)$ is the self-energy of the ith ring, Eq. (26), and the potential $U(r_i,\vec{\lambda}_i;r_j,\vec{\lambda}_j)$ represents the hard ''core'' interaction between ith and jth rings. The integration measure over the radii, $d\mu(r_i)$, is taken to be dr_i. This seems to be a natural choice in view of the mapping from the original problem to this hard ring system.

Now, as we mentioned above, we assume that the fluctuation in $h_i=r_i^2/R$, for all the dimples present, gives a good measure of the shape fluctuation of the sphere itself, for a ''proper'' range of temperatures which will be clarified shortly. Therefore, from now on, we will concentrate on this hard ring system. First, if we neglect the hard-rim interactions between rings, then the partition function is easily integrated.

$$Z_0=\frac{1}{N!d^{3N}}\prod_{i=1}^{N}\int_{r_{\min}}^{r_{\max}} dr_i\int d\vec{\lambda}_i e^{-\beta F(r_i)}, \tag{40}$$

where $r_{\min}=d$ is introduced as an ultraviolet cutoff. As was explained in Sec. IV, d provides the minimum length scale in this picture. Defining $\int d\vec{\lambda}\equiv V$, we obtain

$$Z_0=\frac{V^N}{N!d^{3N}}\prod_{i=1}^{N}\int_{d}^{\infty} dr_i e^{-\beta\kappa r_i^3}\approx\frac{1}{N!}\left(\frac{V}{d^2}\frac{e^{-\beta\kappa d^3}}{\beta\kappa d^3}\right)^N, \tag{41}$$

where we assumed the temperature is low enough to replace $r_{\max}$ ($\ll R$) by ∞. κd^3 provides the elementary energy scale in this model, as in the original problem. [See the discussion below Eq. (28).]

Now, by extremizing the free energy $G=-\beta^{-1}\ln Z$ with respect to the number of rings N, we obtain

$$N_0=\frac{V}{d^2}\frac{e^{-\beta\kappa d^3}}{\beta\kappa d^3}, \tag{42}$$

$$-\beta G_0=N_0. \tag{43}$$

Recalling the thermodynamic relation $G=-PV$ when the chemical potential is identically zero, this is just an ideal gas equation as it should be. Note, however, that P remains constant independent of the volume V.

At a very low temperature, the average number of dimples will be very small compared to V/d^2, and hence the probability of two dimples overlapping will be low. Therefore this phantom ring system should be adequate to describe the low-temperature phase. When $\beta^{-1}\lesssim\kappa d^3$, the average height (or rather depth) of the deformation due to the dimples can be estimated by multiplying the minimum height $h=d^2/R$ by the average area covered by dimples, N_0d^2/V. That is,

$$\langle w\rangle=\frac{d^2}{R}\frac{e^{-\beta\kappa d^3}}{\beta\kappa d^3}. \tag{44}$$

Hence the radius of the *vesicle* is reduced from R to $R-\langle w\rangle$ due to thermal fluctuations. The high-temperature behavior is similarly obtained with the following result for the average height increase:

$$\langle w\rangle=\frac{d^2}{R}\frac{1}{\beta\kappa d^3}. \tag{45}$$

Since $d\sim R^{1/2}$ and $\kappa\sim R^{-5/2}$, $\langle w\rangle$ has an overall linear dependence on R at high temperatures in contrast with the linear case, Eq. (22). This means that the membrane is wildly fluctuating due to this buckling mode, if we do not include the interactions between the dimples.

B. Variational solution

We studied noninteracting gas of rings in Sec. V A, and it is clear that at a high temperature the rings will proliferate, and hence we need to include the ''excluded volume interaction'' between them. We incorporate this hard-rim interaction using a variational method as follows.

First, we define the *one-body distribution function*

$$\rho(r,\vec{\lambda})\equiv\left\langle\sum_{i=1}^{N}\delta(r-r_i)\,\delta(\vec{\lambda}-\vec{\lambda}_i)\right\rangle. \tag{46}$$

Integrating this over r gives the number density of dimples, N/V, which is independent of position for a homogeneous system, and by integrating over the sphere we obtain the *radius distribution function*

$$\rho(r)\equiv\int d\vec{\lambda}\rho(r,\vec{\lambda})=\left\langle\sum_{i=1}^{N}\delta(r-r_i)\right\rangle. \tag{47}$$

We can easily obtain this function at low temperature using the ideal dimple gas approximation

$$\rho_0(r)=\frac{V}{d^3}e^{-\beta\kappa r^3}. \tag{48}$$

The distribution function $\rho(r)$ has all the necessary pieces of information regarding properties of single rings. Among others, one can compute the average size of a ring as well as its higher moments. For example,

$$\langle r_i\rangle_0\equiv\int_d^\infty dr\ r\rho_0(r)\Big/\int_d^\infty dr\ \rho_0(r)=d\left(1+\frac{1}{\beta\kappa d^3}\right), \tag{49}$$

where the subscripts i and 0 indicate that the average is taken for a single ring at low temperature. We note, in passing, that the radius of a dimple increases exponentially when the temperature is raised from $\beta^{-1}=0$.

Now we include the hard-rim interaction in the calculation of the free energy through the variational method using $\rho(r)$. First recall that the system has N dimples on average, and that each dimple has a radius r with the probability $\rho(r)/N$. Then we neglect the fluctuations in $\rho(r)$ and consider a system of N dimples of fixed radii with the distribution $\rho(r)$. We apply a Flory-type argument [33] and obtain the following free energy:

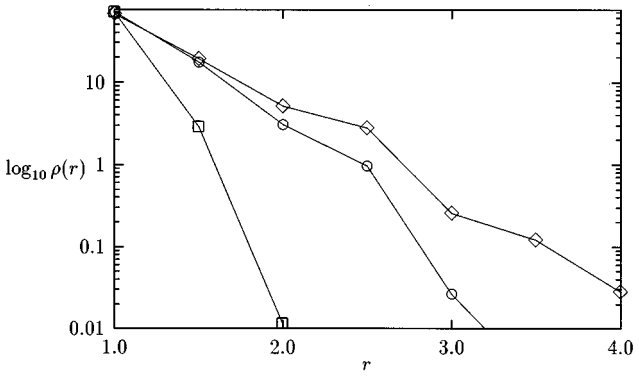

FIG. 4. $\log_{10}\rho(r)$ vs r at $\beta=0$ ($\diamond$), $\beta=0.1$ ($\bigcirc$), and $\beta=1$ ($\square$). The system size is 30×30. The systematic wiggling of data points is due to the presence of a lattice as explained in the text.

$$G=E-\beta^{-1}S, \tag{50}$$

where

$$E=\kappa\int dr\ r^3\rho(r) \tag{51}$$

$$S=-\int dr\ \rho(r)\ln\left(\frac{\rho(r)d^3}{eV}\right)-\frac{2\pi}{V}\left(\int dr\ r\rho(r)\right)^2. \tag{52}$$

Note that this variational free energy G has the form of Virial expansion to second order.

We minimize the free energy with respect to $\rho(r)$, and obtain the following results at high temperature:

$$\rho(r)=\frac{\mathcal{V}}{d^3}e^{-\beta\kappa r^3-r/d}, \tag{53}$$

$$N=\frac{V}{d^2}e^{-\beta\kappa d^3}. \tag{54}$$

As the temperature grows to infinity, the average number N approaches V/d^2 asymptotically. $\rho(r)$ takes a simple exponential form $(V/d^3)e^{-r/d}$.

We performed a computer simulation on a square lattice with periodic boundary conditions. The lattice constant was taken as unity as well as κ. The diameter of a ring was discretized to take only integer values. The minimum radius was set to 1. The system sizes were restricted to 20×20 or 30×30, because the maximum diameter of a ring was around 10 even at $\beta=0$.

The radius distribution function $\rho(r)$ is plotted in Fig. 4 for $\beta=0$, 0.1, and 1 from the top. Even though there are not enough number of data points due to the underlying lattice, the transition from the exponential decay at high temperature to faster than exponential at low temperatures is clearly visible. The oscillations in the plots are due to the fact that we allowed half-integer values for radii.

The average number of dimples is shown in Fig. 5, and the average radius of a single ring is plotted in Fig. 6. As can be seen from these figures, the number of dimples increases

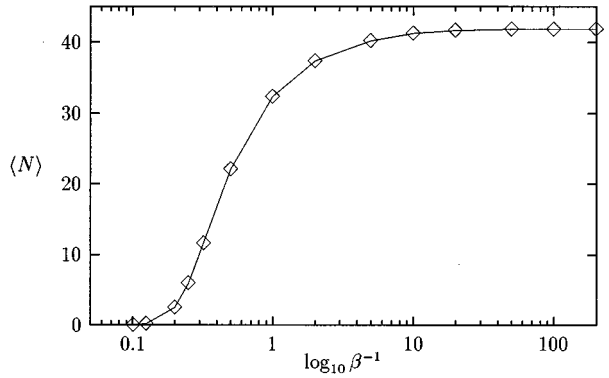

FIG. 5. $\langle N\rangle$ vs $\log_{10}\beta^{-1}$. The system size is 20×20. The error bars are about the size of the symbols. This curve is to be compared with Eq. (54), which predicts the low-temperature exponential growth and the less steep saturation at high temperature.

explosively around $\beta^{-1}=1$, while the size of an individual dimple remains almost constant. The number of dimples saturates as soon as the temperature rises above $\beta^{-1}=1$. The saturation value 40 is about the maximum number of rings with which one can pack in the 20×20 system. The interesting thing is that the average size of rings still grows around $\beta^{-1}=10$ with the total number of rings constant. This also saturates above $\beta^{-1}=100$.

Now we calculate the average height of this deformation due to buckling using simple counting as was done in Sec. V A. This is only possible because the radius of each ring saturates at a fixed value as shown in the simulation. The result is

$$\langle w\rangle=\frac{d^2}{R}e^{-\beta\kappa d^3}. \tag{55}$$

This should be compared with the low-temperature behavior of the phantom ring system, Eq. (44), in which the exponential factor is also dominant. In contrast, Eq. (55) saturates to a fixed value at a high temperature unlike Eq. (45). It should be noted that the saturation value d^2/R is of the same order as the thickness t. Hence, noting that $\langle w\rangle$ is the upper bound for Δw, we conclude that the vesicle remains almost perfectly spherical even at very high temperatures.

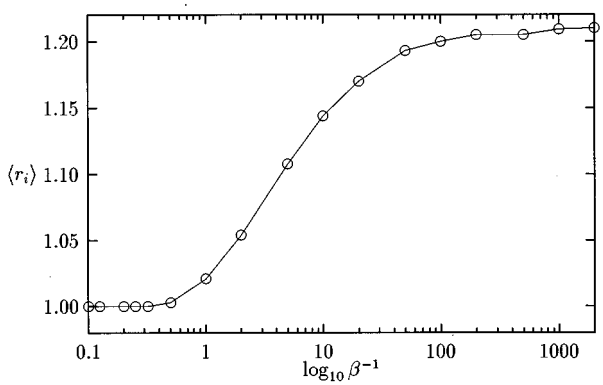

FIG. 6. $\langle r_i\rangle$ vs $\log_{10}\beta^{-1}$. The system size is 20×20. The error bars are about the size of the symbols. The average radius of the rings increases about 20% when the temperature grows one hundredfold from $\beta^{-1}=1$.

Before we close this section, there is one last comment regarding the calculation of $\langle w \rangle$. Due to the presence of nested dimples the average radius of the dimples is not directly related to the height change. For example, the first-level dimple contributes positively to w whereas the second-level dimple contributes negatively. However, as we saw in the variational solution and the simulation results, the average sizes of the dimples are very small, hence the probability of having nested ones are exponentially small.

VI. CONCLUSION

Mechanical and thermodynamical properties of polymerized vesicles have recently attracted a lot of attention due to their relevance to biology and biotechnology. In general, polymerized membranes are very inextensible and flexible at the same time. We studied the shape fluctuations of a closed spherical membrane in this limit. We first showed that one needs to go beyond the linear theory to account for the fluctuations. We then claimed that the dimplelike localized deformation could be a building block of the nonlinear theory. The obvious advantage of this approach is that the actual calculation is done in the linear regime.

For a red blood cell membrane with radius $R=10^{-4}$ m and thickness $t=10^{-8}$ m, we showed that, beyond the length scale $d\sim10^{-6}$ m and the temperature $\beta^{-1}\sim1$ K, the fluctuation of the membrane is well accounted for in terms of the thermodynamic properties of the system of nonoverlapping rings which represent the buckled regions. As it turns out, the spherical membrane remains rigid even though it is made of a very flexible material. This is due to the entropic interaction between thermally generated hard rings. Our theory can be easily verified by light-scattering experiments in the visible spectrum range. We are currently trying to calculate the structure factors for fluctuating spheres. This, however, requires a more elaborate formalism than presented here since we need to calculate Δw directly. Even though we have considered only spherical membranes in this paper, a generalization to arbitrary curved membranes should be straightforward, and the idea of localized nonlinear deformation should still be useful.

ACKNOWLEDGMENTS

This work was supported by NSF Grant No. DMR-9419362, and acknowledgment is made to the Donors of the Petroleum Research Fund, administered by the American Chemical Society, for partial support of this research.

[1] Y. Kantor, M. Kardar, and D. R. Nelson, Phys. Rev. Lett. **57**, 791 (1986).
[2] J. A. Aronovitz and T. C. Lubensky, Phys. Rev. Lett. **60**, 2634 (1988).
[3] E. Guitter, F. David, S. Leibler, and L. Peliti, J. Phys. (France) **50**, 1787 (1989).
[4] R. Lipowsky and M. Girardet, Phys. Rev. Lett. **65**, 2893 (1990).
[5] H. Ringsdorf, B. Schlarb, and J. Venzmer, Angew. Chem. **27**, 113 (1988).
[6] A. Elgsaeter, B. T. Stokke, A. Mikkelsen, and D. Branton, Science **234**, 1217 (1986).
[7] C. F. Schmidt *et al.*, Science **259**, 952 (1993).
[8] M. A. Peterson, H. Strey, and E. Sackmann, J. Phys. (France) II **2**, 1273 (1992).
[9] F. David and E. Guitter, Europhys. Lett. **5**, 709 (1988).
[10] A. Baumgärtner, J. Phys. I **1**, 1549 (1991).
[11] A. Baumgärtner and W. Renz, Europhys. Lett. **17**, 381 (1992).
[12] M. S. Spector, E. Naranjo, S. Chiruvolu, and J. A. Zasadzinski, Phys. Rev. Lett. **73**, 2867 (1994).
[13] D. Bensimon, M. Mutz, and T. Gulik, Physica A **194**, 190 (1993).
[14] D. Liu and M. Plischke, Phys. Rev. A **45**, 7139 (1992).
[15] D. M. Kroll and G. Gompper, J. Phys. (France) I **3**, 1131 (1993).
[16] S. I. Stupp, S. Son, H. C. Lin, and L. S. Li, Science **259**, 59 (1993).
[17] T. Hwa, E. Kokufuta, and T. Tanaka, Phys. Rev. A **44**, R2235 (1991).
[18] X. Wen *et al.*, Nature (London) **355**, 426 (1992).
[19] L. D. Landau and E. M. Lifshitz, *Theory of Elasticity*, 2nd ed. Course of Theoretical Physics, Vol. 7 (Pergamon, Oxford, 1970).
[20] M. A. Peterson, J. Math. Phys. (N.Y.) **26**, 711 (1985).
[21] L. Radzihovsky and J. Toner (unpublished).
[22] A. Lobkovsky *et al.* (unpublished).
[23] S. Komura and R. Lipowsky, J. Phys. (France) II **2**, 1563 (1992).
[24] Z. Zhang, H. T. Davis, and D. M. Kroll, Phys. Rev. E **48**, R651 (1993).
[25] I. B. Petsche and G. S. Grest, J. Phys. (France) I **1**, 1741 (1993).
[26] T. A. Witten and H. Li, Europhys. Lett. **23**, 51 (1993).
[27] L. Bourdieu *et al.*, Phys. Rev. Lett. **72**, 1502 (1994).
[28] B. O'Neill, *Elementary Differential Geometry* (Academic, San Diego, 1966).
[29] A. E. Green and W. Zerna, *Theoretical Elasticity*, 2nd ed. (Oxford University Press, Oxford, 1968).
[30] J. Spanier and K. B. Oldham, *An Atlas of Functions* (Hemisphere, Washington, D.C., 1987).
[31] B. Alberts *et al.*, *Molecular Biology of the Cell*, 2nd ed. (Garland, New York, USA, 1989).
[32] M. Kraus, U. Seifert, and R. Lipowsky (unpublished).
[33] P.-G. de Gennes, *Scaling Concepts in Polymer Physics* (Cornell University Press, Ithaca, NY, 1979).